

Synthesis and Characterization of Tungsten Oxide Sponge like Sub-Microstructures in the Presence Of Novel Surfactants

R. Priya¹, M. Sethu Raman², N. Senthilkumar³, R. Balan⁴

^{1,2,3} Department of Physics, Sri Ramakrishna Mission Vidyalaya College of Arts and Science, Coimbatore 641 020 Tamil Nadu, India

⁴ Department of Physics, KTVR Knowledge park for Engineering and Technology, Coimbatore 641 019, Tamil Nadu, India

Abstract: Tungsten trioxide (WO₃) nanostructures were synthesized by precipitation method using *sodium tungstate dihydrate* (Na₂WO₄·2H₂O) in the presence of surfactant CTAB and PEG-6000. X-ray diffraction, scanning electron microscope, UV-Vis spectroscopy and thermo-gravimetric and differential thermal analysis (TG-DTA) were used to characterize the final product. XRD analysis revealed the presence of an amorphous structure for as-prepared WO₃ nanoparticles. On the other hand, XRD showed formation of a crystalline WO₃ structure with annealing at higher temperature. SEM results depicted the presence of sponge-like sub-microstructure. UV-Vis spectroscopy shows the average reflectance of about 61% in visible region and about 51% in near-infrared region. The calculated optical band gap value is 2.98 eV. The process of decomposition of this system is investigated by TG-DTA.

Keywords: Tungsten oxide nanoparticles, Structural properties, Optical properties.

1. Introduction

In the recent years, the benefits of transition metal oxides have been exploited in many challenging fields of information science, nano and micro-electronics, computer science, energy, transportation, safety engineering, military technologies, optoelectronic, electro chromic devices etc [1]-[2]. Among them one of the most interesting and novel properties of tungsten oxide (WO₃) is applied in advanced technological applications, because of a unique physical and chemical properties, structural transformation and sub-stoichiometric phase transitions and a wide band gap oxide semiconductor properties. It attracted the more attention of researchers to explore their applications in the fields of in electrochromic devices, semiconductor gas sensors and photocatalyses [3]-[4].

The novel properties of nanostructure WO₃ can be prepared by several methods such as template assisted growth [4], anodization [5], conventional thermal evaporation [6], hot wall chemical vapor deposition [7], arc discharge [8], pulsed laser deposition [9], hydrothermal method [10] and solvothermal method [11]. These methods are used to grow all shapes of nanocrystals, including spherical and nanospherical particles, wires, films, disks, rods and thin plates, or voids of sizes in the nanometer range. Among these methods surfactant-assisted chemical co-precipitation is more effective, because of their low temperature growth, less complicated and preparing large scale of size controllable nanoparticles. Surfactants take part an important roles in crystallization process and also it will control the growth and agglomeration. In this present work, we investigated surfactant effect on synthesized as-prepared and annealed tungsten oxide nanoparticles structural characterization, morphology, thermal decomposition and optical properties.

2. Experimental

2.1 Synthesis of WO₃ Sponge-Like Submicrostructure

The WO₃ nanoparticles were synthesized by dissolving sodium tungstate dihydrate in deionised water solution with stirring. The solution was mixed with oxalic acid (1M), CTAB (1g) and PEG-6000 (0.5g) and hydrochloric acid (HCl) was separately dissolved with deionised water and added one by one to the precursor solution with stirring. The final solution was heated to 80°C for 1 hour, to ensure complete reaction. The milky white precipitation obtained and several times washed with de-ionized water, ethanol and acetone to remove unreactant compound. Finally, the precipitated powder was collected and then dried at 60°C in an oven for 6 hours, which was later found to be an amorphous WO₃ and therefore designated as AWS. Then the samples were annealed in muffle furnace at 400°C for 1 hour was to confirm the crystallization of WO₃ and denoted as SW.

2.2 Characterization

The synthesized WO₃ samples were characterized of their structure carried out using a bruker AXS D8 Advanced X-Ray diffraction meter. A scanning electron microscope (VEGA3 TESCAN) was used to analysis the surface morphology at 30 kV. Optical measurements were carried out in UV-Vis spectrophotometer (SHIMADZU 3600 UV-Vis-NIR spectrophotometer), the weight changes of the WO₃ material in relation to temperature changes were revealed by Simultaneous Differential Thermal Analysis (STDA).

3. Results and Discussion

3.1. Structural characteristics of WO₃

Structural analysis reveals to understand the crystallinity and phase purity of the nanoparticles. Fig. 1 represents the XRD patterns of two different specimens namely ASW and SW. As mentioned earlier, the powder of ASW obtained immediately after the oven drying and observed to be an amorphous in nature (Fig. 1a). XRD patterns of the annealed SW powders confirm their crystalline nature with monoclinic structure (Fig. 2b). The monoclinic structure of SW with XRD peaks correspond to (0 1 1), (0 0 2), (1 2 0), (1 1 2), (0 2 2), (0 2 3), (0 1 4), (1 4 1), (4 1 2), (2 4 2), (5 0 1), (6 0 0) and (0 4 5) planes. The most intense peak was observed at (0 0 2) plane. The interplanar spacing “d” were calculated by using different peaks represent in diffractogram and compared with standard values.

The crystallite sizes of both SW specimens can be evaluated using the Scherrer’s equation [12]:

$$D = \frac{0.9\lambda}{\beta \cos \theta} \text{----- (1)}$$

where D is the crystallite size (nm), λ is the wavelength of the X-ray, θ is the Bragg’s angle and β is the full width at half maximum (FWHM) of the diffraction peak at 2θ. The maximum crystallite size of SW was found to be 67.53 nm at 400°C.

The lattice constants ‘a’, ‘b’ and ‘c’ were calculated using the following equation:

$$\frac{1}{d^2} = \frac{1}{\sin^2 \beta} \left(\frac{h^2}{a^2} + \frac{k^2 \sin^2 \beta}{b^2} + \frac{l^2}{c^2} - \frac{2hl \cos \beta}{ac} \right) \text{---- (2)}$$

where, a, b and c are the monoclinic lattice (a=b=c) parameters. In this relation (h, k, l) are miller indices of reflector planes appearing on the diffraction spectra and d_{hkl} their inter-reticular distances. The lattice constants are found

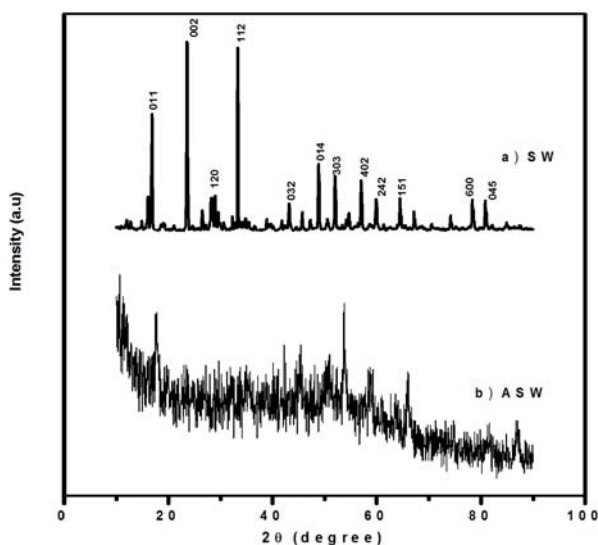


Figure 1: XRD spectra of as-prepared (a) amorphous WO₃ (ASW) and (b) annealed sponge – like WO₃ (SW) at 400°C to be a=7.324 Å, b=7.59 Å and c=7.53 Å, results are in good agreement with the standard values taken from the JCPDS card No. 72-1465

3.2 Morphology Analysis of WO₃ Nanoparticles

The SEM micrographs of the as-prepared and the annealed WO₃ powder at 400°C temperatures are shown in Fig. 2 (a)–(b). Fig (2a) describes that water-cleaned and dried as-prepared ASW powder has partly spherical and irregular shape particles aggregated in the surface. The fig 2(b) SEM image shows the formation of sponge-like sub- micro-structures of WO₃ at 400°C [13]. The CTAB and PEG-6000 surfactants play an important role to the formation of the

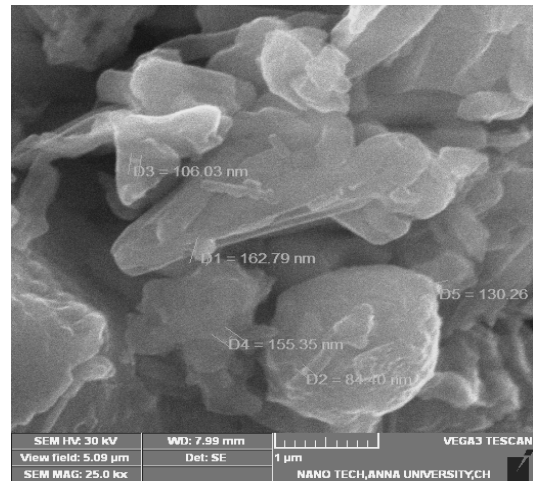


Figure 2 a: SEM image of ASW

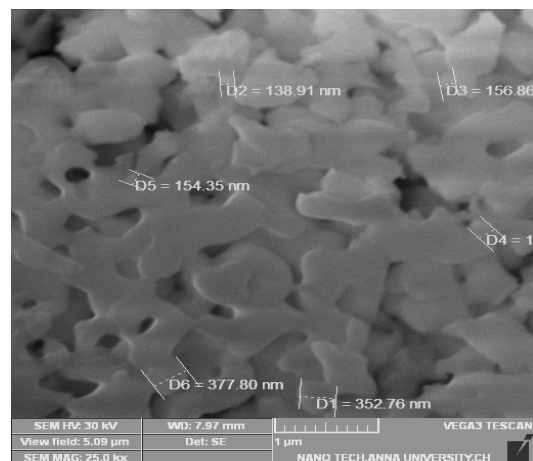


Figure 2 b: SEM image of SW

irregular sponge like submicro-structure aggregated with size in the range of 138 nm. SEM micrographs describe the morphology transformation from amorphous to crystallite WO₃ at 400°C.

3.3 Thermal Analysis

The simultaneous differential thermal analysis (STDA) of the amorphous WO₃ samples was carried out upto 1000 °C with a heating rate of 2°C/min. The thermogram of amorphous (ASW) WO₃ in Fig. 3 describes high instability of the compound due to the presence of both physisorbed and chemisorbed water [14]. Thermo-gravimetric weight loss at 100°C is close to 3 wt% and additional 5 wt% weight loss is due to removal of physisorbed and chemisorbed water molecule from tungsten oxide powder. It is observed that no further weight loss occurred beyond 400°C. In DSC, endothermic peak is attributed to the loss of physisorbed and

chemisorbed water. The exothermic peak at 300°C represents the changes of tungsten oxide phase from amorphous to

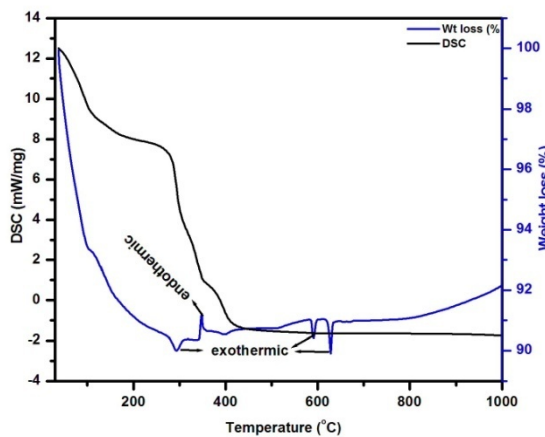


Figure 3: TG-DSC of amorphous WO₃ (ASW) powders

crystalline under a dynamic condition. These results suggest that the amorphous WO₃ is formed at around 300°C with the removal of water molecules. The same is crystallized at a temperature 400°C with exothermic peak. This analysis confirms the favour of formation of crystalline WO₃ at a temperature of 400°C.

3.4 Optical Properties

Fig. 4 (a, b) shows the optical absorption and reflection for as-prepared (ASW) and annealed WO₃ (SW) with wavelength range 200-1000 nm. This figure indicates two effects: (a) a shift of the absorption edge depends on the sample temperature and (b) the reflectance of the sample shifts towards higher wavelength side at a higher temperature [16]. The as-prepared (ASW) and sponge-like sub-microstructure WO₃ (SW) sample has maximum absorption value in the UV region and decreases sharply with increasing wavelength and becomes almost constant towards the visible and middle IR region. The percentage of reflection of ASW and SW decreases to zero in the UV region and increases to 62 % and 46 % in the visible region respectively. The sponge-like sub-microstructure (SW) has maximum absorption and reflectance compared to as-prepared WO₃ (ASW).

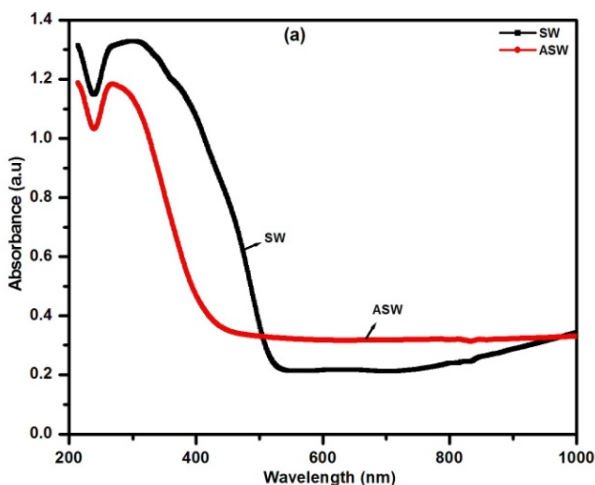


Figure 4: (a) Optical absorbance spectra of ASW and SW

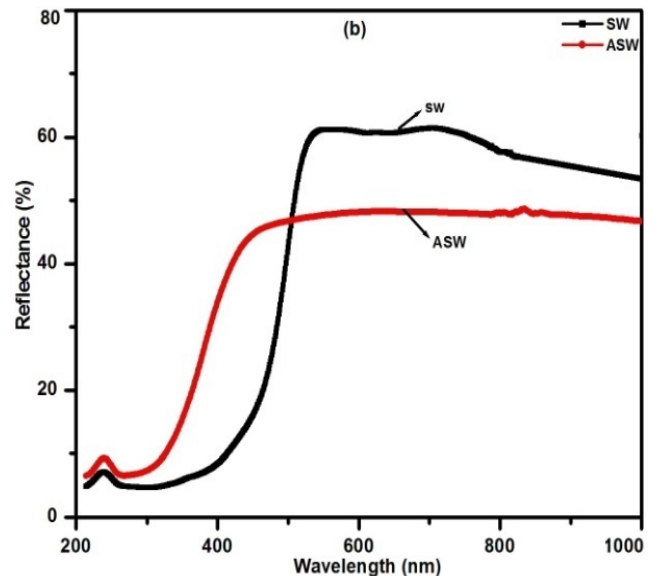


Figure 4: (b) Reflection spectra of ASW and SW

The optical band gap of both the samples can be calculated from Kubelka-Munk function. The Kubelka - Munk function (KM) is used to convert reflectance measurements (R) into equivalent absorption spectra [16].

$$KM = \frac{(1 - R)^2}{2R} \text{-----(3)}$$

The optical band gap (E_g) values are obtained by extrapolating the linear portion of the plots of $(\alpha h\nu)^{1/2}$ with $h\nu$ of the samples as shown in Fig. 4 (c). The optical band gap of annealed WO₃ (SW) is found to be 2.98 eV. These optical indirect band gap values are in good agreement with the reports [17]. The band gap value of as-prepared tungsten oxide (ASW) describes insulating property.

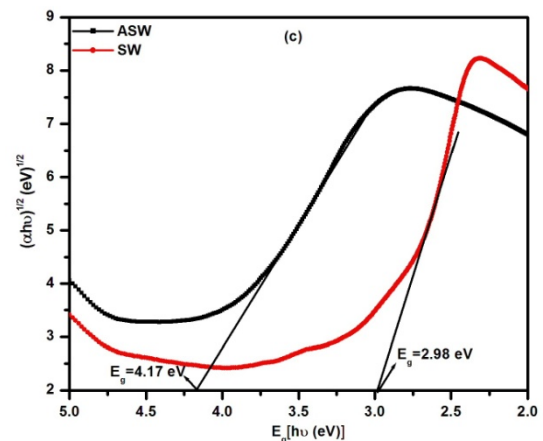


Figure 4: (c) Optical band gap (E_g) of ASW and SW

4. Conclusions

Nanocrystalline, uniform and irregular sponge-like sub-microstructure and amorphous tungsten oxide was successfully grown by simple surfactant assisted co-precipitation method using sodium tungstate dihydrate as the source material with surfactants CTAB and PEG. The surfactants play an important role to control the particle size. For the reaction, the particle was initially amorphous but become crystalline on annealed at a temperature of 400°C. The annealed tungsten oxide powder has polycrystalline

nature with most prominent (002) reflection. The calculated crystalline size was found to be 67.53 nm. From STDA analysis, the first step reaction removes the small amount of hydroxyl ion present in the resultant powder by heating to a temperature of 200°C. Second step reaction confirms the crystalline phase of tungsten oxide at a temperature of 400°C. The optical study shows that the reflectance (61%) of tungsten oxide is high in the visible region. The observed indirect band gap value of annealed WO₃ is 2.98 eV, which can be used as potential application in solar cell.

References

- [1] N. Prabhua, S. Agilanb, N. Muthukumarasamy, C.K. Senthilkumar "Effect of Temperature on The Structural and Optical Properties of WO₃ Nanoparticles Prepared by Solvo Thermal Method" Digest Journal of Nanomaterials and Biostructures, (8), pp. 1483 – 1490, 2013.
- [2] Vijay Bhooshan Kumar and Dambarudhar Mohanta "Formation of Nanoscale Tungsten Oxide Structures and Colouration Characteristics" Bull. Mater. Sci., Indian Academy of Sciences, (34), pp. 435–442, 2011.
- [3] C. Santato, M. Odziemkowski, M. Ulmann and J. Augustynski "Crystallographically Oriented Mesoporous WO₃ Films: Synthesis, Characterization, and Applications", J. Am. Chem. Soc. 123, pp. 10639–10649, 2001.
- [4] D.Z. Guo, K. Yu-Zhang, A. Glote, G.M. Zhang and Z.Q. Xue "Synthesis and Characterization of Tungsten Oxide Nanorods", J. Mater. Res., (19) pp. 3665–3670, 2004.
- [5] M. Sadakane, K. Sasaki, H. Kunioku, B. Ohtani, W. Ueda, R. Abe, "Preparation of Nano-Structured Crystalline Tungsten(VI) Oxide and Enhanced Photocatalytic Activity for Decomposition of Organic Compounds under Visible Light Irradiation", Chem. Commun., (48), pp. 6552–6554, 2008.
- [6] A.A. Mozalev, V. Khatko, C. Bittencourt, A.W. Hassel, G. Gorokh, E. Llobet, X. Correig "Nanostructured Tungsten Oxide Semiconductor Prepared by Anodic and Thermal Processing of Al/W/Ti Thin-Film Layers", Chem. Mater., (20), pp. 6482–6493, 2008.
- [7] B. Cao, J. Chen, X. Tang, W. Zhou, "Growth of monoclinic WO₃ nanowire array for highly sensitive NO₂ detection", J. Mater. Chem., (19), pp. 2323–2327, 2009.
- [8] Y. Zhang, Y. Chen, H. Liu, Y. Zhou, R. Li, M. Cai, X. Sun, "3D Hierarchical Structure of Single Crystalline Tungsten Oxide Nanowires: Construction, Phase Transition and Voltammetric Behavior", J. Phys. Chem., (113), pp. 1746–1750, 2009.
- [9] A.A. Ashkarran, A. Irajizad, M.M. Ahadian, S.A.M. Ardakani, "Synthesis and Photocatalytic Activity of WO₃ Nanoparticles Prepared by The Arc Discharge Method in Deionized Water", Nanotechnology, (19), pp. 195709, 2008.
- [10] K.J. Lethy, D. Beena, V.P. Mahadevan Pillai, V. Ganesan, "Bandgap Renormalization in Titania Modified Nanostructured Tungsten Oxide Thin Films Prepared by Pulsed Laser Deposition Technique For Solar Cell Applications", J. Appl. Phys., (104-3), pp. 033515–12, 2008.
- [11] S. Rajagopal, D. Nataraj, D. Mangalaraj, YahiaDjaoued Jacques Robichaud, O. Yu. Khyzhun "Controlled Growth of WO₃ Nanostructures with Three Different Morphologies and Their Structural Optical and Photodecomposition Studies", Nanoscale. Res. Lett., (4), pp. 1335–1342, 2009.
- [12] Hong Goo Choi, Young Hwa Jung, and Do Kyung Kim "Solvothermal Synthesis of Tungsten Oxide Nanorod/Nanowire/Nanosheet" J. Am. Ceram. Soc., (88-6), pp. 1684–1686, 2005.
- [13] Yue Wang, Yong-Fang Shi, Yu-Biao Chen, Li-Ming Wu, "Hydrazine reduction of metal ions to porous submicro-structures of Ag, Pd, Cu, Ni, and Bi", Journal of Solid State Chemistry, (191), pp. 19–26, 2012.
- [14] Z. Wang, X. Hu, "Electrochromic properties of TiO₂-doped WO₃ films", Electrochim Acta, (46), pp. 1951–1956, 2001.
- [15] K.J. Patel, C.J. Panchal, V.A. Kheraj, M.S. Desai, "Growth, Structural, Electrical and Optical Properties of The Thermally Evaporated Tungsten Trioxide (WO₃) Thin Films", Materials Chemistry and Physics, (114), pp. 475, 2009.
- [16] P. Kubelka, F. Munk, "Ein Beitrag zur Optik der Farbanstriche", Z. Tech. Phys. (Leipzig) (12), pp. 593–601, 1931.
- [17] R. Sivakumar, C. Sanjeeviraja, M. Jayachandran, R. Gopalakrishnan, S.N. Sarangi, D. Paramanik, T. Som, "Modification of WO₃ thin films by MeV N⁺-ion beam irradiation", Journal of Physics-Condensed Matter, (19), pp. 186204, 2007.